BLIND CFO ESTIMATION FOR OFDM WITH CONSTANT MODULUS CONSTELLATIONS: PERFORMANCE BOUNDS AND ALGORITHMS

Timo Roman, Andreas Richter, and Visa Koivunen

SMARAD CoE, Signal Processing Laboratory, Helsinki University of Technology
P.O. Box 3000, FIN-02015 HUT, Finland
Email: {troman, arichter, visa}@wooster.hut.fi

ABSTRACT

In this paper, we derive the Cramér-Rao bound for blind carrier frequency offset (CFO) estimation in orthogonal frequency division multiplexing (OFDM) with constant modulus constellations. A blind maximum likelihood CFO estimator is also proposed. It achieves highly accurate frequency synchronization with a single OFDM block, regardless of multipath fading and without the need for null-subcarriers. The approach is thus very attractive for time and frequency (i.e., doubly) selective channels where the CFO may be time varying. If sufficient additional pilot information is available, maximum likelihood estimates of channel parameters and transmitted data can be obtained as a byproduct. Finally, performance bounds are evaluated for several commonly encountered scenarios.

1. INTRODUCTION

Orthogonal Frequency Division Multiplexing (OFDM) is a powerful technique to handle impairments of wireless communication channels such as multipath propagation. Hence, OFDM is a viable candidate for future 4G wireless communications techniques. However, OFDM and multicarrier modulation in general are highly sensitive to carrier frequency synchronization errors caused by oscillator inaccuracies and Doppler shifts due to mobility [1]. Carrier frequency offset (CFO) leads to intercarrier interference (ICI) which severely degrades the performance. Therefore, CFO compensation must be accomplished with high fidelity in time and frequency selective wireless channels.

In practice, distinguishing the pilots from the information-bearing symbols is difficult due to the nonlinear distortion caused by the CFO. Here, blind estimators may provide an appealing alternative [2, 3, 4]. They allow efficient decoupling of the carrier frequency synchronization problem from both channel estimation and data detection. Those tasks may then be performed as subsequent steps.

In this paper, we first derive the Cramér-Rao bound (CRB) for the blind CFO estimation problem in OFDM systems using constant modulus symbols. The CRB defines the smallest achievable variance among the class of unbiased estimators. Hence, it is an important performance measure. The stochastic CRB for the above problem was derived in [5, 6] under the circular or non-circular complex Gaussian approximation. Despite the approximation, the related bound does not provide clear indication on the CFO estimation performance for a particular channel and data sequence. For this purpose, we follow the deterministic approach. The related CRB is referred to as conditional or deterministic CRB. Assuming constant modulus (CM) modulations, the CFO is shown to be identifiable without any null-subcarrier (NSC), i.e., even in the case when all the subcarriers are active. The CRBs on the channel magnitude and phase parameters are obtained as well.

Based on the knowledge of the structure of the Fisher information matrix (FIM), we propose a novel maximum likelihood (ML) estimator for the CFO as well as the channel magnitude and phase parameters. The new blind ML estimator for the CFO outperforms the algorithms in [3, 4]. The proposed estimator needs only a single OFDM block to obtain reliable estimates under time and frequency selective fading, unlike most of the blind techniques, which commonly require extensive time averaging. For these reasons, the proposed method is particularly suited to doubly selective channels. The key idea is to exploit correlation among OFDM subcarriers and more specifically in the magnitude squared spectrum of the channel [3, 4]. Furthermore, we use a parametrization which does not lead to a rank deficient FIM, i.e., the parameters are identifiable. Simulation studies demonstrate that the projection based estimators [3, 4] perform close to their respective CRBs.

The rest of the paper is organized as follows. The parametric model for the OFDM system is described in Section 2. The CRB is derived in Section 3. Section 4 introduces the blind ML estimator. Simulation results are reported in Section 5. Finally, Section 6 concludes the paper.

2. SYSTEM MODEL

Let us assume an OFDM transmission with N_a modulated subcarriers out of a total of N, and consider a single block of data for simplicity. Assuming perfect symbol timing, the received OFDM signal in time domain after cyclic prefix removal, including the frequency offset, is expressed as

$$\mathbf{y} = \beta \mathbf{C}_\epsilon \mathbf{F} \mathbf{V} \mathbf{D}_{\tilde{\mathbf{h}}} \mathbf{a} + \mathbf{w}, \tag{1}$$

where $\mathbf{y}$ is a $N \times 1$ vector, $\beta = \sqrt{N/N_a}$ ensures that the total transmitted power is constant regardless of N_a, and $\mathbf{F}$ is the unitary $N \times N$ inverse discrete Fourier transform (IDFT) matrix. The diagonal matrix $\mathbf{C}_\epsilon$ introduces the frequency offset and is defined as

$$\mathbf{C}_\epsilon = e^{j2\pi\epsilon L_{\text{CP}}/N} \cdot \text{diag}\left\{1, \ldots, e^{j2\pi\epsilon(N-1)/N}\right\}, \tag{2}$$

where L_{CP} is the length of the cyclic prefix ($L_{\text{CP}} < N$) and diag$\{\}$ denotes the diagonal matrix constructed from the argument vector. The quantity $\epsilon \in [0, 1[$ is referred to as normalized frequency offset wrt. intercarrier spacing. The (m,n) element of the $N \times N_a$ tall selection matrix $\mathbf{V}$ is 1 if the n^{th} symbol is transmitted on the m^{th} subcarrier, and zero otherwise [1]. The $N_a \times N_a$ diagonal matrix $\mathbf{D}_{\tilde{\mathbf{h}}}$ in (1) contains the channel frequency response $\tilde{\mathbf{h}} = [\tilde{h}_{n_1}, \ldots, \tilde{h}_{n_{N_a}}]^T$ at active subcarriers frequencies on its main diagonal, and $\mathcal{N}_{\text{A}} = \{n_1, \ldots, n_{N_a}\} \in \{0, \ldots, N-1\}$ is the subset of active subcarrier indices. A block fading channel model is considered. The CFO is assumed to vary block-wise as well. Moreover, when viewed as part of the channel, the CFO renders the channel time-variant over the duration of an OFDM block. Thus, this model clearly applies to doubly-selective channels. The vector $\mathbf{a} = [a_{n_1}, \ldots, a_{n_{N_a}}]^T$ of size $N_a \times 1$ contains constant modulus symbols, i.e., $|a_n|^2 = 1, \forall n \in \mathcal{N}_{\text{A}}$. The complex noise term $\mathbf{w}$ is assumed to be zero-mean circular complex Gaussian with covariance matrix $\sigma^2\mathbf{I}$.

3. CRAMÉR-RAO BOUND FOR BLIND CFO ESTIMATION WITH CM MODULATIONS

3.1 Parametrization of the channel magnitude spectrum

The channel frequency response (CFR) at active subcarriers is related via discrete Fourier transform to a L_h-tap channel impulse response (CIR) in time domain as follows:

$$\tilde{h}_n = \sum_{l=0}^{L_h-1} h_l e^{j2\pi ln/N}, \quad n \in \mathcal{N}_{\text{A}}, \tag{3}$$

where $h_0, \ldots, h_{L_h-1}$ are the CIR coefficients in time domain ($L_h \leq L_{\text{CP}} + 1$). It is shown in [3] that the squared magnitude $|\tilde{h}_n|^2$ of the CFR may be parametrized as

$$\begin{aligned}
|\tilde{h}_n|^2 &= \mathbf{c}_n^T \boldsymbol{\lambda}, \quad n \in \mathcal{N}_{\text{A}} \\
\mathbf{c}_n &= \sqrt{2}\Big[\tfrac{1}{\sqrt{2}}, \cos\left(\tfrac{2\pi n}{N}\right), \ldots, \cos\left(\tfrac{2\pi n(L_h-1)}{N}\right), \\
&\qquad \sin\left(\tfrac{2\pi n}{N}\right), \ldots, \sin\left(\tfrac{2\pi n(L_h-1)}{N}\right)\Big]^T \in \mathbb{R}^{2L_h-1\times 1} \\
\boldsymbol{\lambda} &= \Big[g_0, \sqrt{2}\,\text{Re}\{g_1\}, \ldots, \sqrt{2}\,\text{Re}\{g_{L_h-1}\}, \\
&\qquad \sqrt{2}\,\text{Im}\{g_1\}, \ldots, \sqrt{2}\,\text{Im}\{g_{L_h-1}\}\Big]^T \in \mathbb{R}^{2L_h-1\times 1} \\
g_i &= \textstyle\sum_{l=0}^{L_h-1-i} h_l^* h_{l+i} \in \mathbb{C},
\end{aligned} \tag{4}$$

where Re{} and Im{} denote the real and imaginary parts, respectively. Hence, the magnitude squared spectrum is entirely characterized by the $2L_h - 1$ channel autocorrelation coefficients in time domain. Notice that the above parametrization is identical to the one used in [4].

3.2 Parametrization for OFDM with CM modulations

Since $\mathbf{a}$ is a vector of CM symbols, the model in (1) for the received signal may be rewritten as

$$\mathbf{y} = \beta \mathbf{C}_\epsilon \mathbf{F}\mathbf{V}\mathbf{D}_{|\tilde{\mathbf{h}}|}\mathbf{v}_{\boldsymbol{\varphi}} + \mathbf{w}, \tag{5}$$

with the following notation:

$$\mathbf{D}_{|\tilde{\mathbf{h}}|} = \text{diag}\{\mathbf{v}_{|\tilde{\mathbf{h}}|}\} \tag{6}$$

$$\mathbf{v}_{|\tilde{\mathbf{h}}|} = [|\tilde{h}_{n_1}|, \ldots, |\tilde{h}_{n_{N_a}}|]^T = \left[\sqrt{\mathbf{c}_{n_1}^T\boldsymbol{\lambda}}, \ldots, \sqrt{\mathbf{c}_{n_{N_a}}^T\boldsymbol{\lambda}}\right]^T \tag{7}$$

$$\mathbf{v}_{\boldsymbol{\varphi}} = \left[e^{j\varphi_{n_1}}, \ldots, e^{j\varphi_{n_{N_a}}}\right]^T, \tag{8}$$

where (7) follows from (4) and $\varphi_n = \arg\{\tilde{h}_n a_n\}$, $n \in \mathcal{N}_{\text{A}}$.

3.3 Likelihood function

Let us stack the real parameters ϵ, $\boldsymbol{\lambda}$, and $\boldsymbol{\varphi}$ into the vector $\boldsymbol{\theta} = \left[\epsilon, \boldsymbol{\lambda}^T, \boldsymbol{\varphi}^T\right]^T$ of length $N_a + 2L_h$.
By defining $\mathbf{s}(\boldsymbol{\theta}) = \beta\mathbf{C}_\epsilon\mathbf{F}\mathbf{V}\mathbf{D}_{|\tilde{\mathbf{h}}|}\mathbf{v}_{\boldsymbol{\varphi}}$, we may rewrite (5) as

$$\mathbf{y} = \mathbf{s}(\boldsymbol{\theta}) + \mathbf{w}. \tag{9}$$

Assuming that the parameter vector $\boldsymbol{\theta}$ is an unknown deterministic quantity, the vector of observations $\mathbf{y}$ is complex circular Gaussian with mean $\mathbf{s}(\boldsymbol{\theta})$ and covariance matrix $\sigma^2\mathbf{I}$. Dropping out the terms independent of $\boldsymbol{\theta}$, the log-likelihood function may be expressed as

$$\mathcal{L}\left(\mathbf{y}|\boldsymbol{\theta}, \sigma^2\right) \propto -\frac{1}{\sigma^2}(\mathbf{y} - \mathbf{s}(\boldsymbol{\theta}))^H(\mathbf{y} - \mathbf{s}(\boldsymbol{\theta})). \tag{10}$$

Notice that optimizing (10) with respect to $\boldsymbol{\theta}$ leads to a nonlinear least-squares problem.

3.4 Fisher information matrix

The Fisher information matrix (FIM) for the deterministic ML (DML) problem in (9) may be expressed as [7, 8]:

$$\begin{aligned}
\boldsymbol{\mathcal{I}}_{\boldsymbol{\theta}} &= \frac{2}{\sigma^2}\text{Re}\left\{\left(\frac{\partial}{\partial\boldsymbol{\theta}^T}\mathbf{s}(\boldsymbol{\theta})\right)^H\left(\frac{\partial}{\partial\boldsymbol{\theta}^T}\mathbf{s}(\boldsymbol{\theta})\right)\right\} && (11)\\
&= \frac{2}{\sigma^2}\text{Re}\left\{\mathbf{J}_{\boldsymbol{\theta}}^H\mathbf{J}_{\boldsymbol{\theta}}\right\} \in \mathbb{R}^{N_a+2L_h\times N_a+2L_h}, && (12)
\end{aligned}$$

where the $N \times N_a + 2L_h$ Jacobian matrix $\mathbf{J}_{\boldsymbol{\theta}}$ is defined as:

$$\mathbf{J}_{\boldsymbol{\theta}} = \left[\frac{\partial}{\partial\epsilon}\mathbf{s}(\boldsymbol{\theta}), \frac{\partial}{\partial\boldsymbol{\lambda}^T}\mathbf{s}(\boldsymbol{\theta}), \frac{\partial}{\partial\boldsymbol{\varphi}^T}\mathbf{s}(\boldsymbol{\theta})\right]. \tag{13}$$

The partial derivatives above are obtained as

$$\begin{aligned}
\frac{\partial}{\partial\epsilon}\mathbf{s}(\boldsymbol{\theta}) &= \beta\bar{\mathbf{C}}_\epsilon\mathbf{F}\mathbf{V}\mathbf{D}_{|\tilde{\mathbf{h}}|}\mathbf{v}_{\boldsymbol{\varphi}} && (14)\\
\frac{\partial}{\partial\boldsymbol{\lambda}^T}\mathbf{s}(\boldsymbol{\theta}) &= \frac{1}{2}\beta\mathbf{C}_\epsilon\mathbf{F}\mathbf{V}\mathbf{D}_{\boldsymbol{\varphi}}\mathbf{D}_{|\tilde{\mathbf{h}}|}^{-1}\mathbf{C}^T && (15)\\
\frac{\partial}{\partial\boldsymbol{\varphi}^T}\mathbf{s}(\boldsymbol{\theta}) &= j\beta\mathbf{C}_\epsilon\mathbf{F}\mathbf{V}\mathbf{D}_{|\tilde{\mathbf{h}}|}\mathbf{D}_{\boldsymbol{\varphi}}, && (16)
\end{aligned}$$

with the following notation:

$$\begin{aligned}
\bar{\mathbf{C}}_\epsilon &= j\frac{2\pi}{N}\text{diag}\{L_{\text{CP}}, \ldots, L_{\text{CP}} + N - 1\} \odot \mathbf{C}_\epsilon && (17)\\
\mathbf{D}_{\boldsymbol{\varphi}} &= \text{diag}\{\mathbf{v}_{\boldsymbol{\varphi}}\} && (18)\\
\mathbf{C} &= \left[\mathbf{c}_{n_1}, \ldots, \mathbf{c}_{n_{N_a}}\right], && (19)
\end{aligned}$$

where $\odot$ stands for the element-wise or Hadamard product.

3.5 Structure of the FIM and the CRB matrix

Let us now take a closer look at the structure of the FIM in (12). It may be partitioned into nine blocks:

$$\boldsymbol{\mathcal{I}}_{\boldsymbol{\theta}} = \begin{bmatrix} \boldsymbol{\mathcal{I}}_{\epsilon,\epsilon} & \boldsymbol{\mathcal{I}}_{\boldsymbol{\lambda},\epsilon}^T & \boldsymbol{\mathcal{I}}_{\boldsymbol{\varphi},\epsilon}^T \\ \boldsymbol{\mathcal{I}}_{\boldsymbol{\lambda},\epsilon} & \boldsymbol{\mathcal{I}}_{\boldsymbol{\lambda},\boldsymbol{\lambda}} & \boldsymbol{\mathcal{I}}_{\boldsymbol{\varphi},\boldsymbol{\lambda}}^T \\ \boldsymbol{\mathcal{I}}_{\boldsymbol{\varphi},\epsilon} & \boldsymbol{\mathcal{I}}_{\boldsymbol{\varphi},\boldsymbol{\lambda}} & \boldsymbol{\mathcal{I}}_{\boldsymbol{\varphi},\boldsymbol{\varphi}} \end{bmatrix}. \tag{20}$$

After some derivations, expressions for the diagonal blocks of the FIM are found:

$$\mathcal{I}_{\epsilon,\epsilon} = 2\gamma \mathbf{v}_{\boldsymbol{\varphi}}^H \mathbf{D}_{|\tilde{\mathbf{h}}|} \mathbf{U} \mathbf{D}_{|\tilde{\mathbf{h}}|} \mathbf{v}_{\boldsymbol{\varphi}} \in \mathbb{R} \tag{21}$$

$$\mathcal{I}_{\boldsymbol{\lambda},\boldsymbol{\lambda}} = \frac{1}{2}\gamma \mathbf{C} \mathbf{D}_{|\tilde{\mathbf{h}}|}^{-2} \mathbf{C}^T \in \mathbb{R}^{2L_h-1\times 2L_h-1} \tag{22}$$

$$\mathcal{I}_{\boldsymbol{\varphi},\boldsymbol{\varphi}} = 2\gamma \mathbf{D}_{|\tilde{\mathbf{h}}|}^2 \in \mathbb{R}^{N_a\times N_a}, \tag{23}$$

where $\mathbf{U} = \frac{4\pi^2}{N^2}\mathbf{V}^T\mathbf{F}^H \operatorname{diag}\left\{L_{\text{CP}}^2, \ldots, (L_{\text{CP}}+N-1)^2\right\}\mathbf{F}\mathbf{V}$. The signal-to-noise ratio (SNR) is defined as $\gamma = \beta^2/\sigma^2$. The off-diagonal blocks of the FIM may be expressed as:

$$\mathcal{I}_{\boldsymbol{\lambda},\epsilon} = \gamma \operatorname{Re}\left\{\mathbf{C}\mathbf{D}_{|\tilde{\mathbf{h}}|}^{-1}\mathbf{D}_{\boldsymbol{\varphi}}^{*}\mathbf{W}\mathbf{D}_{|\tilde{\mathbf{h}}|}\mathbf{v}_{\boldsymbol{\varphi}}\right\} \in \mathbb{R}^{2L_h-1\times 1} \tag{24}$$

$$\mathcal{I}_{\boldsymbol{\varphi},\epsilon} = 2\gamma \operatorname{Re}\left\{-j\mathbf{D}_{\boldsymbol{\varphi}}^{*}\mathbf{D}_{|\tilde{\mathbf{h}}|}\mathbf{W}\mathbf{D}_{|\tilde{\mathbf{h}}|}\mathbf{v}_{\boldsymbol{\varphi}}\right\} \in \mathbb{R}^{N_a\times 1} \tag{25}$$

$$\mathcal{I}_{\boldsymbol{\varphi},\boldsymbol{\lambda}} = \mathbf{0}_{N_a\times 2L_h-1}, \tag{26}$$

with $\mathbf{W} = j\frac{2\pi}{N}\mathbf{V}^T\mathbf{F}^H \operatorname{diag}\{L_{\text{CP}}, \ldots, L_{\text{CP}}+N-1\}\mathbf{F}\mathbf{V}$. Now, the following remarks are in order:

1. The FIM does not depend on the value ϵ of the CFO.
2. There is no coupling between the channel magnitude squared parameters $\boldsymbol{\lambda}$ and the phase parameters $\boldsymbol{\varphi}$.
3. The information on the CFO ϵ is coupled with all the other parameters.
4. The phase parameters $\boldsymbol{\varphi}$ are not mutually coupled, i.e., $\mathcal{I}_{\boldsymbol{\varphi},\boldsymbol{\varphi}}$ is a diagonal matrix. This relates to the orthogonality of the OFDM transmission scheme.
5. The channel magnitude squared parameters $\boldsymbol{\lambda}$ exhibit coupling.

Finally, the CRB matrix $\mathcal{C}$ as well the individual CRBs on the parameters ϵ, $\boldsymbol{\lambda}$ and $\boldsymbol{\varphi}$ are obtained as:

$$\begin{array}{lcll} \mathcal{C} & = & \mathcal{I}_{\boldsymbol{\theta}}^{-1} & \\ \mathcal{C}_{\epsilon} & = & \{\mathcal{C}\}_{1,1} & \\ \mathcal{C}_{\lambda_i} & = & \{\mathcal{C}\}_{1+i,1+i}, & i = 1,\ldots,2L_h-1 \\ \mathcal{C}_{\varphi_i} & = & \{\mathcal{C}\}_{2L_h+i,2L_h+i}, & i = 1,\ldots,N_a, \end{array} \tag{27}$$

where $\{\mathcal{C}\}_{m,n}$ stands for the (m,n) element of the CRB matrix and λ_i (resp. φ_i) denotes the i^{th} element of the vector $\boldsymbol{\lambda}$ (resp. $\boldsymbol{\varphi}$). A pictorial representation of the FIM and the CRB matrix is given in Figure 1. A remarkable property is that the error on λ_1 is uncorrelated with the error on the CFO and the phase parameters. Indeed, λ_1 represents the total channel energy (i.e., $\|\mathbf{h}\|^2$, see (4)), which may be estimated regardless of the CFO or the CM symbols.

Notice that the parametrization in (5) guarantees the identifiability of the parameters, i.e., the FIM is invertible, provided that $N_a \geq L_h$ [3]. The model in (1) leads to a phase ambiguity and a rank deficient FIM: the phase of the channel parameters may not be distinguished from that of the symbols without any additional pilot information. Assuming a perfectly compensated CFO, L_h pilots symbols are needed to fully estimate the channel coefficients and then recover the transmitted data. One may eventually circumvent the problem by looking for a constrained CRB [9]. However, a proper constraint still remains to be found.

4. BLIND MAXIMUM LIKELIHOOD ESTIMATION

Given the log-likelihood function in (10), maximum likelihood estimates of channel magnitude, phase and CFO parameters may be obtained as

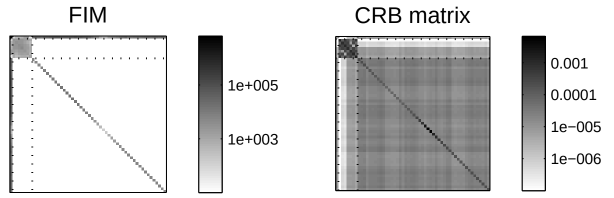

Figure 1: Structure of the FIM and the CRB matrix for $N = 64$, $N_a = 48$, and $L_h = 4$. Dark colors correspond to high absolute values and white areas to zeros. Blocks are delimited by dotted lines.

$$\hat{\boldsymbol{\theta}}_{\text{ML}} = \arg\max_{\boldsymbol{\theta}} \mathcal{L}\left(\mathbf{y}|\boldsymbol{\theta},\sigma^2\right). \tag{28}$$

The likelihood function is a nonlinear function of the parameter vector $\boldsymbol{\theta}$. The Levenberg-Marquardt algorithm is the method of choice for nonlinear least-square problems [10]. In our case, it proceeds as follows. At iteration i, the score function needs to be evaluated first:

$$\mathbf{q}\left(\mathbf{y}|\hat{\boldsymbol{\theta}}^{\{i\}},\sigma^2\right) = \frac{2}{\sigma^2}\operatorname{Re}\left\{\hat{\boldsymbol{\theta}}^{\{i\}^H}\left(\mathbf{y}-\mathbf{s}\left(\hat{\boldsymbol{\theta}}^{\{i\}}\right)\right)\right\}. \tag{29}$$

The estimated parameter vector is then iteratively updated as follows:

$$\hat{\boldsymbol{\theta}}^{\{i+1\}} = \hat{\boldsymbol{\theta}}^{\{i\}} + \left(\mathcal{I}_{\hat{\boldsymbol{\theta}}^{\{i\}}} + \zeta^{\{i\}}\mathcal{I}_{\hat{\boldsymbol{\theta}}^{\{i\}}} \odot \mathbf{I}\right)^{-1}\mathbf{q}\left(\mathbf{y}|\hat{\boldsymbol{\theta}}^{\{i\}},\sigma^2\right), \tag{30}$$

where the step size $\zeta^{\{i\}}$ at iteration i is chosen such that the update stays within the trust region [10].

As the likelihood function may have several local minima, the parameters need to be initialized properly in order to find the global optimum. For this purpose, we follow the procedure below:

1. Obtain initial $\hat{\epsilon}^{\{0\}}$, e.g. by using the algorithms in [3, 4].
2. Compensate for the CFO using $\hat{\epsilon}^{\{0\}}$ and form the carrier-synchronized signal estimate in the frequency domain at active subcarriers: $\hat{\tilde{\mathbf{y}}} = \mathbf{V}^T\mathbf{F}^H\mathbf{C}_{\hat{\epsilon}^{\{0\}}}^{*}\mathbf{y}$.
3. Obtain an estimate of the magnitude squared spectrum at active subcarriers: $\hat{\mathbf{v}}_{|\tilde{\mathbf{h}}|^2} = \frac{1}{\beta^2}\hat{\tilde{\mathbf{y}}} \odot \hat{\tilde{\mathbf{y}}}^*$.
4. Initialize $\hat{\boldsymbol{\lambda}}^{\{0\}}$ and $\hat{\boldsymbol{\varphi}}^{\{0\}}$ respectively as:
   $\hat{\boldsymbol{\lambda}}^{\{0\}} = \beta^2\mathbf{C}\hat{\mathbf{v}}_{|\tilde{\mathbf{h}}|^2}$
   $\hat{\boldsymbol{\varphi}}^{\{0\}} = [\hat{\varphi}_{n_1}^{\{0\}}, \ldots, \hat{\varphi}_{n_{N_a}}^{\{0\}}]^T$, $\hat{\varphi}_n^{\{0\}} = \arg\{\hat{\tilde{y}}_n\}$, $n \in \mathcal{N}_{\text{A}}$.

The algorithms [3, 4] used at step 1 to initialize the CFO parameter are very close to the ML solution, as will be demonstrated in simulations next. Consequently, the initialization problem reduces to the estimation of the channel magnitude and phase parameters. Since the FIM for $\boldsymbol{\lambda}$ and $\boldsymbol{\varphi}$ is a block diagonal matrix, initial estimates for both parameters may be computed independently as it is done in step 4. Hence, the above procedure provides a reliable way for initializing the ML algorithm.

The major computational cost lies in the calculation of the matrix inverse in (30). Given the special structure of the

FIM (see Section 3.5 and Fig. 1), the inverse may be found with significantly lower complexity by exploiting the properties of partitioned matrices. The number of required operations in both cases is proportional to:

- Conventional inversion: $N_a^3 + 8L_h^3 + 6N_a^2 L_h + 12N_a L_h^2$.
- Partitioned inversion: $N_a^2 + 16L_h^3 + 4N_a L_h - 12L_h^2$.

Typically $L_h \ll N_a$, and thus the complexity may be reduced almost by a factor of N_a.

5. SIMULATION RESULTS

The simulation results are reported in this section. The total number of subcarriers is set to $N = 64$ and the length of the cyclic prefix is $L_{\text{CP}} = 4$. QPSK modulation is used. The normalized frequency offset is set as $\epsilon = 0.43$. We choose the same deterministic four-tap channel impulse response as in [6] in order to allow a comparison with the CRB. The channel is unknown to the receiver whereas its length L_h is assumed to be known a-priori. In practice, it may either be estimated or upper-bounded by the length of the cyclic prefix [4]. A single OFDM block is used for the estimation of the parameters of interest. It is assumed to remain unchanged in all the simulations. The mean square error (MSE), $\text{MSE} = \text{E}\left[|\hat{\epsilon} - \epsilon|^2\right]$, is chosen as the error criterion for carrier frequency offset estimation. Empirical MSEs are ensemble averages over 10000 realizations of the noise process. Depending on the use of null-subcarriers, the two following scenarios are considered:

I. $N_a = 64$ active subcarriers, no null-subcarrier.
II. $N_a = 48$ active subcarriers, $N_z = 16$ equispaced NSCs.

The CRB on the carrier frequency offset derived in (27) for OFDM using CM constellations is plotted in Figure 2 for scenarios I and II. The curves are referred to as 'CM' and 'NSC+CM', respectively. In addition, the deterministic CRB on the CFO derived in [1] is also shown for comparison. It applies to OFDM systems transmitting non-CM symbols in the presence of NSCs and is referred to as 'CRB (NSC)'. In our specific simulation case, the CM property without NSCs provides 1.5 dB gain over the system with NSCs and non-CM symbols, and 3 dB gain if both NSCs and CM symbols are used. Also, note that the CRB curves are dependent on the placement of the null-subcarriers (if any), as well as on the transmitted symbol and the channel impulse response [1].

Let us now consider scenario I and compare the MSE performance of the two following algorithms in Figure 3:

I-1 The projection-based blind CFO estimator of [4] exploiting the CM property (denoted 'Proj. (CM)').
I-2 The proposed blind ML estimator (denoted 'ML (CM)') described by equations (28)-(30). The 'CM' algorithm is used to initialize the CFO estimate (Section 4, step 1).

While the blind CFO estimator of [4] lies 1 dB above the CRB, the proposed blind ML estimator achieves the bound for SNRs larger than 10 dB. In practice, no more than five iterations of the Levenberg-Marquardt algorithm are needed.

We now consider the scenario II and compare in Figure 4 the MSE performance of the three following algorithms:

II-1 The blind CFO estimator of [2] based on NSCs solely (denoted 'NSC').
II-2 The blind CFO estimator of [3] exploiting jointly NSCs and the CM property (denoted 'NSC+CM').

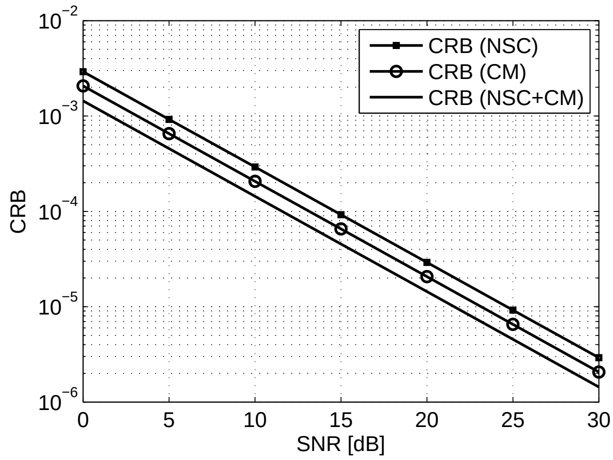

Figure 2: CRB vs. SNR for different signal models. A gain of 1.5 dB over the NSC case is achieved by exploiting the CM property. A 3 dB gain is obtained if both NSCs and CM symbols are present.

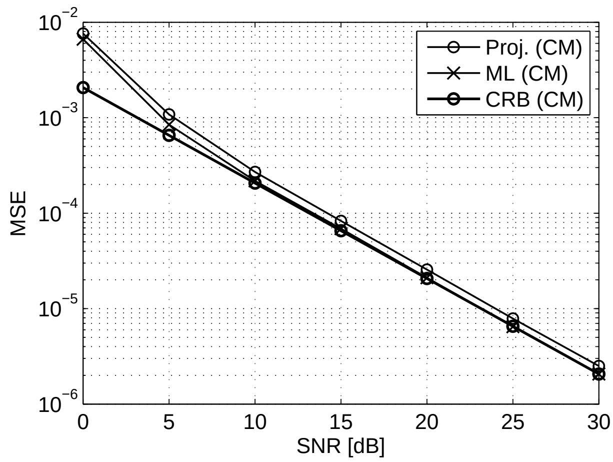

Figure 3: MSE of the projection based CM blind CFO estimator [4] and the proposed blind ML CFO estimator. The ML estimator closes the 1 dB gap between [4] and the CRB. The CRB is attained for a single OFDM block and SNRs larger than 10 dB.

II-3 The proposed blind ML estimator (denoted 'ML (NSC+CM)'). The 'NSC+CM' algorithm is used to provide an initial estimate for the CFO (Section 4, step 1).

The blind ML estimator achieves the CRB for values of the SNR above 10 dB. Also, the gap of the method in [3] to the CRB is negligible. On the other hand, the NSC-based estimator achieves the CRB only when constant modulus symbols are not in use. Otherwise, a 3 dB loss is experienced.

Both the projection based 'CM' estimator [4] and the joint 'NSC+CM' criterion [3] perform extremely close to their respective CRBs in practice. This is not surprising since both algorithms are closely related to maximum likelihood estimation [3]. The estimation error on the CFO is well below 1% wrt. intercarrier spacing at 15 dB SNR, while a tolerance of 5% is commonly considered to be sufficient for QPSK modulation in practical systems [1]. Also, no error

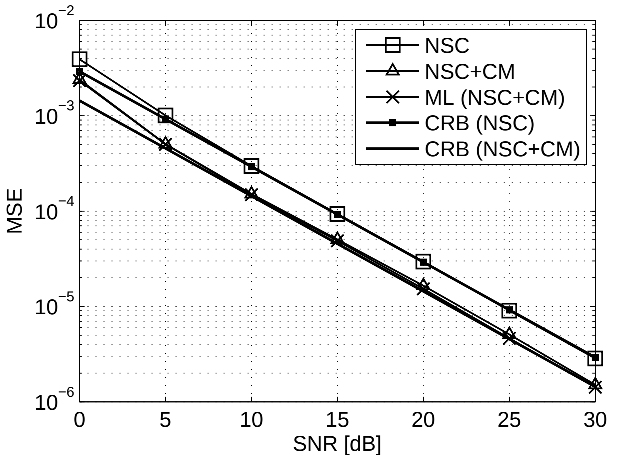

Figure 4: MSE of the NSC [2], NSC+CM [3] and proposed blind ML CFO estimator. The CRB is attained by the ML estimator for a single OFDM block and SNRs larger than 10 dB. It is observed that [3] is very close to the ML solution. Almost 3 dB gain is achieved over the NSC algorithm [2].

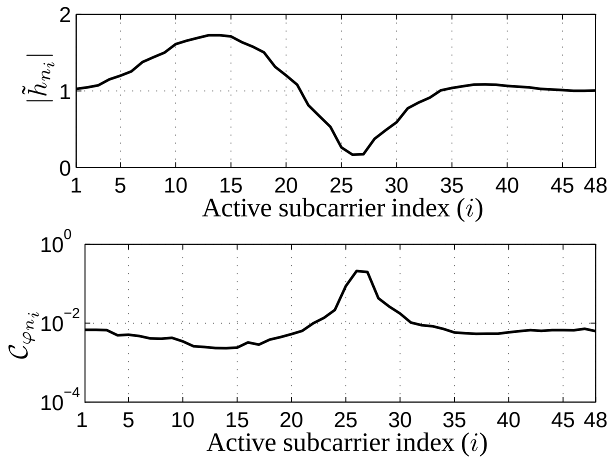

Figure 5: *Upper plot:* Channel magnitude spectrum at active subcarrier frequencies. *Lower plot:* CRB on the phase parameters at 15 dB SNR. The CRBs for the phase parameters are approximately inversely proportional the channel magnitude spectrum, which determines the SNR on the subcarriers.

floor is observed in MSE and hence the proposed estimators are unbiased. Moreover, the algorithms in [3, 4] proved to be a reliable way to initialize the ML estimator in practice, as explained in Section 4. The algorithms in [3, 4] are computationally less complex than the proposed ML estimator since they involve one-dimensional search of the value of the CFO only. On the other hand, the ML algorithm provides information on the channel magnitude and phase parameters, which are later needed for equalization purposes, once frequency synchronization has been performed. The MSE curves for magnitude and phase parameter ML estimation are not shown, due to the lack of space. However, they converge to their respective CRBs as well.

Finally, for a given SNR, we may also study the individual CRBs on the phase parameters as a function of the subcarrier index. The results are presented in Figure 5. The CRBs are approximately inversely proportional to the channel magnitude spectrum which determines the SNR on the subcarriers. The CRBs on the phase parameters are of high importance as the final objective is to transmit information through the system.

6. CONCLUSIONS

In this paper, we derived the Cramér-Rao bound for blind carrier frequency offset estimation in OFDM using constant modulus constellations. The performance of existing blind CFO estimators exploiting the CM property is compared to the obtained CRB. A blind maximum likelihood CFO estimator is also proposed. The estimator achieves the CRB with a single OFDM block, regardless of multipath fading and without the need for null-subcarriers or training. The approach is thus very attractive for doubly selective channels where the CFO may be time varying. If additional information is available, maximum likelihood estimates of channel parameters and transmitted data may be obtained as a byproduct.

REFERENCES

[1] M. Ghogho and A. Swami, “Carrier frequency synchronization for OFDM systems,” in *Signal Processing for mobile communications handbook* (M. Ibnkahla, ed.), ch. 8, CRC Press, 2005.

[2] U. Tureli, H. Liu, and M. Zoltowski, “OFDM blind carrier offset estimation: ESPRIT,” *IEEE Transactions on Communications*, vol. 48, pp. 1459–1461, Sept. 2000.

[3] M. Ghogho and A. Swami, “Blind frequency-offset estimator for OFDM systems transmitting constant-modulus symbols,” *IEEE Communications Letters*, vol. 6, pp. 343–345, Aug. 2002.

[4] T. Roman and V. Koivunen, “Subspace method for blind CFO estimation for OFDM systems with constant modulus constellations,” in *Proc. of the IEEE Vehicular Technology Conference*, vol. 2, pp. 1253–1257, May 2005.

[5] P. Ciblat and M. Ghogho, “Harmonic retrieval in non-circular complex-valued multiplicative noise: Cramér-Rao bound,” in *Proc. of the IEEE International Conference on Acoustics, Speech, and Signal Processing*, vol. 2, pp. II 489–II 492, May 2004.

[6] T. Roman, S. Visuri, and V. Koivunen, “Performance bound for blind CFO estimation in OFDM with real-valued constellations,” in *Proc. of the IEEE Semiannual Vehicular Technology Fall Conference*, vol. 6, pp. 3866–3870, Sept. 2004.

[7] P. Stoica, A. Jakobsson, and J. Li, “Cisoid parameter estimation in the colored noise case: asymptotic Cramér-Rao bound, maximum likelihood, and nonlinear least-squares,” *IEEE Transactions on Signal Processing*, vol. 45, pp. 2048–2059, Aug. 1997.

[8] S. Kay, *Fundamentals of Statistical Signal Processing - Estimation Theory*. Englewood Cliffs, NJ, Prentice Hall, 1993.

[9] P. Stoica and B. Ng, “On the Cramér-Rao bound under parametric constraints,” *IEEE Signal Processing Letters*, vol. 5, pp. 177–179, Jul. 1998.

[10] J. Moré, “The Levenberg-Marquardt algorithm: implementation and theory,” in *Proc. of the Dundee Conference on Numerical Analysis*, pp. 105–116, 1978.